MRI For Response Assessment In Oncologic Bone Marrow Lesions

F. Lecouvet, P. Omoumi, A. Larbi, B. Tombal, N. Michoux, B. Vande Berg, M. Lonneux, and J. Malghem

Contents

Abstract

Imaging has multiple roles in oncology. Besides lesion detection and characterization, disease staging, the quantification of the tumor load and the evaluation of response to therapy are of critical importance for the patient and for the clinician, both in primary and metastatic cancers. The assessment of the response to treatment of bone lesions has been considered difficult or impossible even for most prestigious cancer authorities, compared to lesions involving soft tissues or other organs like the lungs or liver, for which response evaluation criteria exist. This is mainly due to the lack of sensitivity, specificity and measurement capabilities of imaging techniques that have been available for years for the assessment of bone lesions, i.e. bone scintigraphy (BS), radiographs and X-ray computed tomography (CT). This chapter first summarizes the possibilities and limitations of the aforementioned techniques. It illustrates the capabilities of "modern" imaging modalities, i.e. positron emission tomography (PET) and most importantly magnetic resonance imaging (MRI). Practical morphologic as well as functional observations that can be made using MRI at primary diagnosis are emphasized as well as the evaluation of response of bone marrow lesions to treatment. Technical advances in MRI, which further refine the capabilities of this modality for early evaluation of the response, including dynamic contrast-enhanced (DCE) imaging and diffusion-weighted imaging (DWI), are also covered.

F. Lecouvet (✉) · P. Omoumi · A. Larbi · N. Michoux · B. Vande Berg · M. Lonneux · J. Malghem
Department of Radiology,
Cliniques Universitaires Saint-Luc,
UCL Université de Louvain,
Hippocrate Avenue, 10/2942,
1200 Brussels, Belgium
e-mail: lecouvet@yahoo.fr

B. Tombal
Department of Urology,
Cliniques Universitaires Saint-Luc,
UCL Université de Louvain,
Hippocrate Avenue, 10/2942,
1200 Brussels, Belgium

A. Baur-Melnyk (ed.), *Magnetic Resonance Imaging of the Bone Marrow*, Medical Radiology. Diagnostic Imaging,
DOI: 10.1007/174_2011_492, © Springer-Verlag Berlin Heidelberg 2013

1 Clinical Background

The assessment of the therapeutic response of neoplastic conditions is of critical importance in the daily practice of oncology and in clinical trials. Both the clinician and the researcher want to know whether their patient's lesions respond to therapy, either to adapt the patient's treatment or to evaluate the benefit of new treatments. Besides clinical and biological tumoral markers, imaging is a fundamental actor in this evaluation of tumor response. Morphologic and functional imaging plays a key role in many cancers for the evaluation of the response to treatment of primary lesions and metastases, using quantitative measurement tools (RECIST, WHO criteria), validated for soft tissue lesions, mainly involving lung, liver, brain, lymph nodes and other organs (Therasse et al. 2000; Eisenhauer et al. 2009). In contrast, there is a critical need for validated monitoring tools in hematologic diseases involving the skeleton and in "osteophilic" cancers (which show a specific tropism for bone in their dissemination). In the absence of monitoring tools for bone disease, the clinician can only rely on "skeletal related events" (SRE) to monitor the disease, which presents well-known limits (Scher et al. 2011). Moreover, the clinician needs endpoints, i.e. prognostic parameters that provide information on the further evolution of the patient and of the disease, for example in terms of complications, progression free survival and overall survival. Among these endpoints, treatment response has been repeatedly demonstrated to be an important determinant of survival, which critically lacks in patients with predominant or exclusive involvement of bones (Sonpavde et al. 2011). Hence, the advent of valuable tools for the evaluation of bone marrow involvement and of the response to therapy generates wide interest among oncologists and hematologists.

2 Available Imaging Techniques: Overview

The historical difficulty of bone assessment results from the characteristics of imaging techniques used until now. Conventional radiography, BS and CT rely on the activation of bone cells—osteoblasts and osteoclasts—to detect changes in bone trabeculae caused by neoplastic lesions. This explains their lack of sensitivity at the early stages of the disease. Other limitations of these techniques are the lack of measurement capabilities, a poor sensitivity to treatment induced changes, and confusing findings such as the "flare phenomenon", that can be misinterpreted as a false progression of the disease.

PET and MRI have proven to be able to detect the neoplastic colonization of bone before the activation of bone cells. PET relies on the affinity of tumor cells for some radiopharmaceuticals and has the great advantage to propose a one step "whole body—all organ" staging. MRI offers excellent sensitivity for the detection of neoplastic cells within the bone marrow using basic anatomic sequences. Most useful sequences are T1-weighted FSE sequences, due to their high sensitivity in detecting fatty marrow replacement by neoplastic colonization, with a high contrast between the low signal intensity of the lesions and the high signal intensity of the surrounding marrow. These sequences are often completed by a fluid-sensitive sequence. The performance of MRI, and its superiority over BS and conventional radio graphy in terms of lesion detection, has been widely demonstrated in metastases from solid cancers and in hematologic malignancies (Daldrup-Link et al. 2001; Eustace et al. 1997; Ghanem et al. 2006; Nakanishi et al. 2005; Yang et al. 2011). Recent advances in hardware and software have lead to the development of sequences that can cover the whole body (WBMRI). The advent of DWI and DCE sequences further boosts this ability to detect and monitor bone lesions, even in anatomic areas of the skeleton that are more difficult to evaluate using conventional sequences (ribs, peripheral bones…), and to monitor their response to therapy (Ghanem et al. 2005; Schmidt et al. 2007).

3 Bone Scintigraphy and Single Photon Emission Computed Tomography

Based on its wide availability, limited cost, and sensitivities and specificities that have been considered acceptable for several decades, BS has been and still remains commonly used for the detection of bone lesions in "osteophilic" cancers (breast, prostate, thyroid, kidney…). The technique is based on the use

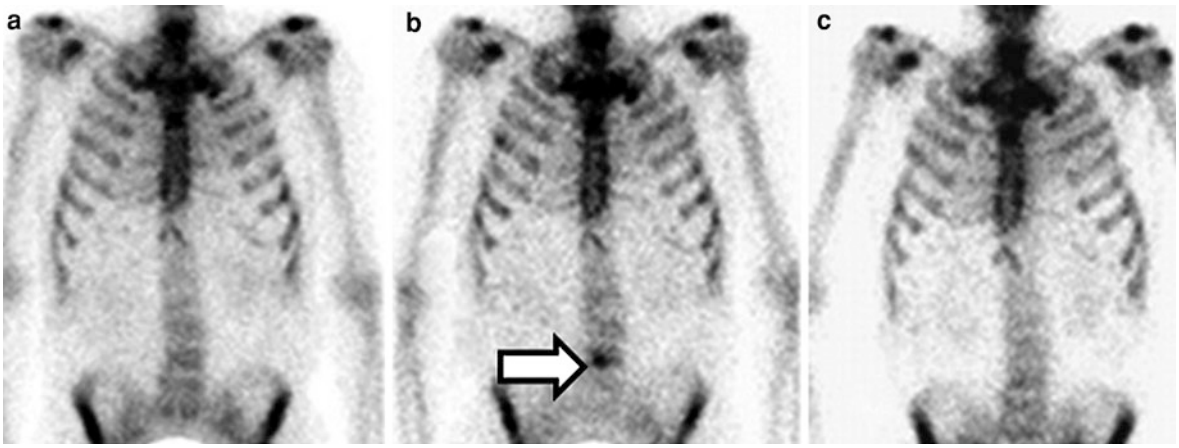

Fig. 1 Illustration of the "flare phenomenon" on consecutive Tc99 m bone scans (BS) in a patient with breast cancer. **a** Initial staging does not reveal any significant uptake. **b** Three-month follow-up BS reveals appearance of a focal uptake (*arrow*), suggesting the appearance of a metastasis. **c** Six-month follow-up BS shows disappearance of this focal abnormality; this observation, and the continuous decrease in seric markers, confirm the "flare phenomenon" observed at three-month follow-up (osteoblastic response within a previously occult BS lesion)

of a tracer (diphosphonate-bound 99 m-Technetium) showing an affinity for osteoblasts. This explains a limited sensitivity, especially in (predominantly) osteolytic bone lesions. Modern imaging techniques (PET and MRI) reveal the presence of lesions in a significant proportion of patients with negative BS, with critical impact on the therapeutic decisions (Avrahami et al. 1989; Balliu et al. 2010; Gosfield et al. 1993). Curative therapy may indeed only be considered if no metastasis is present; if metastases are present, systemic treatment is required.

Since BS is a marker of osteoblastic activity, its specificity is also limited, with frequent uptake in benign conditions such as degenerative joint diseases, benign fractures or Paget disease. This often raises the need for second line examinations to clarify BS findings, most often radiographs, which may leave the radiologist with a residual doubt, leading to the discussion of third line imaging modalities (CT or MRI) when radiographs do not provide neither a typical benign nor a frank malignant explanation to the abnormal uptake seen on the BS (discrepancy between negative BS and positive radiographs). This multistep approach raises evident questions of costs, time, irradiation and convenience for the patient (Lecouvet et al. 2007).

In terms of response assessment, BS is even more insufficient, not only due to its lack of sensitivity and specificity, but most importantly due to its lack of spatial resolution and measurement capabilities, and delay for detecting significant changes or even disease resolution, compared to other clinical parameters of response or progression (Condon et al. 1981; Scher 2003).

Moreover, BS findings after treatment may be falsely positive for disease progression. The "flare phenomenon" is characterized by the appearance of new abnormalities or enlargement of previous pathologic foci, due to an osteoblastic response, i.e. new bone formation within pre-existing, and sometimes occult lesions, which respond to therapy and are wrongly considered as new or progressive lesions (Ciray et al. 2000; Venkitaraman et al. 2009). The correct identification of this transient phenomenon is only made a posteriori on the follow-up BS that shows fading of the falsely progressive lesions, often more than 6 months after treatment response (Pollen et al. 1984) (Fig. 1). This phenomenon is not uncommon, with reported frequencies of 6–25% in patients with prostate cancer metastases, and in 33% of patients with treated breast metastases (Messiou et al. 2009).

Single-photon emission computed tomography (SPECT), now most commonly combined with CT technology, improves the anatomic resolution and reduces the number of equivocal and false positive findings compared to BS. However, SPECT remains limited in terms of sensitivity and provides significant irradiation (Even-Sapir et al. 2006; Savelli et al. 2001). Its role in lesion follow-up under treatment also remains to be evaluated.

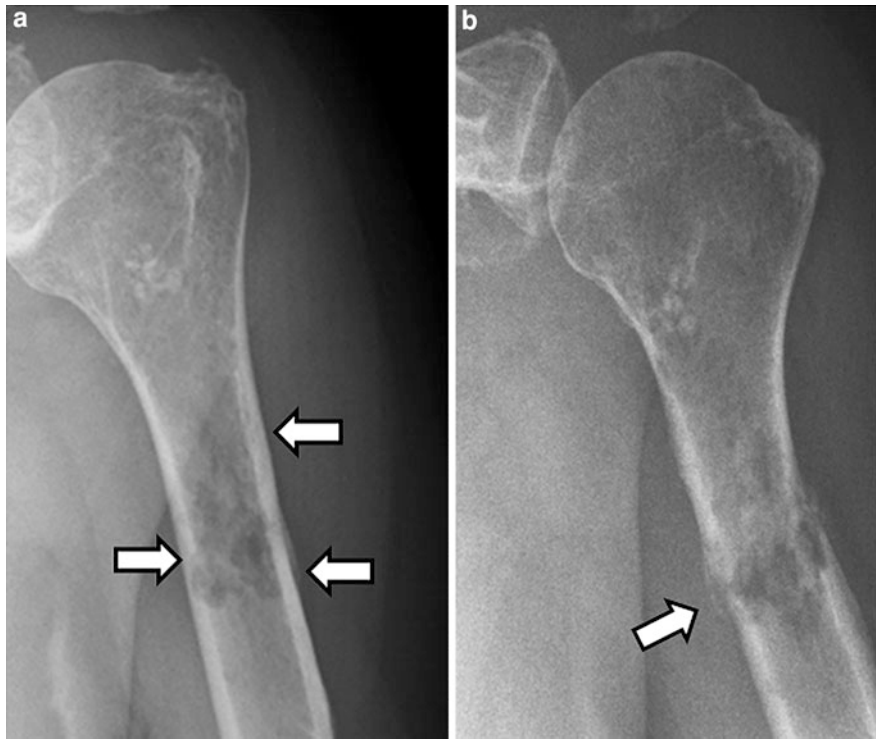

Fig. 2 Radiographic diagnosis of a pathologic fracture. **a** Radiograph of the left humerus obtained because of scintigraphic uptake shows lytic lesion (*arrows*) within the diaphysis typical for a metastasis. **b** Two weeks later, radiograph performed in the emergency room because of acute spontaneous pain reveals pathologic fracture (*arrow*)

4 Radiography

Radiography remains the first line tool for investigating painful skeletal areas and for the positive diagnosis of pathologic fractures once they have occurred, in patients with or without known cancer or bone involvement (Fig. 2). There is no role for radiographs in the setting of a systematic screening for neoplastic bone lesions, except for multiple myeloma (MM) (cf. infra). They have indeed a low sensitivity, especially for the detection of lytic lesions within the trabecular bone, which require 30–75% bone loss before being detectable (Vinholes et al. 1996).

In metastatic disease, their main role is the clarification of a nonspecific or equivocal BS finding, the evaluation of the either osteolytic or osteoblastic "behavior" of a lesion and the evaluation of the fracture risk associated with lesions detected by BS, PET or MRI.

The observation of radiographic signs of therapeutic response of bone lesions—peripheral sclerosis, lesion filling and condensation—is often delayed by several months, ambiguous or absent despite clinical improvement, which explains that there is no place for X-rays in the systematic evaluation of response (Coombes et al. 1983; Galasko 1995; Hamaoka et al. 2004; Libshitz and Hortobagyi 1981).

In multiple myeloma (MM), radiographs are still used in most centers for the staging (Durie and Salmon), while its replacement by MRI is commonly advocated for an earlier detection of lesions associated with (a risk of evolution to) an advanced stage of disease (Durie 2006; Lecouvet et al. 1999). This radiographic survey has a limited value for disease follow-up, as the comparison with MRI clearly demonstrates the frequent persisting visibility of lytic areas on radiographs despite evident signs of response based on the bone marrow signal changes at MRI (Baur-Melnyk et al. 2005; Moulopoulos et al. 1994).

5 Computed Tomography

As this technique is irradiating, CT exploration is generally targeted to a definite portion of the body and is not used as a tool for systematic bone screening in cancer. This might be reconsidered over the years due to the advent of multidetector CT (MDCT)-based whole body capabilities and consistent efforts to reduce the radiation doses necessary to achieve

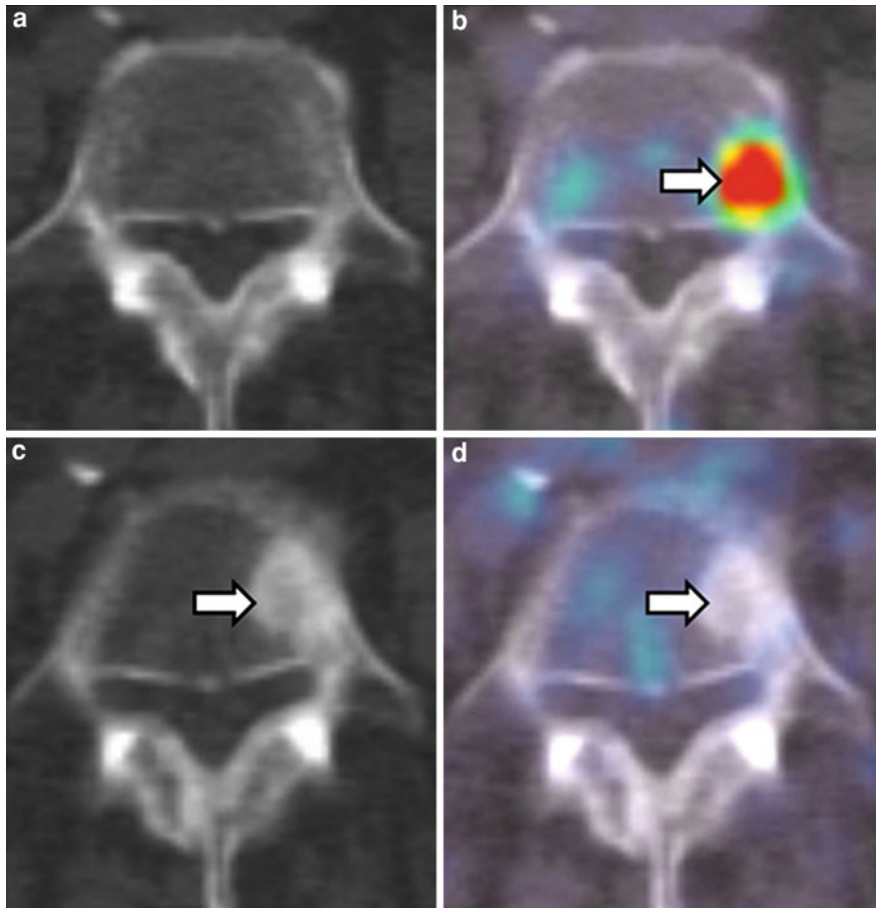

Fig. 3 18FDG-PET/CT correlation at diagnosis (**a**, **b**) and after treatment (**c**, **d**) in a patient with breast cancer. (**a**, **b**) At diagnosis, CT does not show any abnormality within this lumbar vertebra despite evident left-sided focus of FDG uptake, typical for a metastasis (*arrow* in **b**). (**c**, **d**) After three cycles of chemotherapy, an osteoblastic focus is evident on the CT (*arrow* in c), which could be mistaken as a new sclerotic metastasis on the basis of the CT; PET shows disappearance of the FDG uptake, indicating responsive lesion (*arrow* in **d**)

sufficient diagnostic information (Hamaoka et al. 2004; Groves et al. 2006; Horger et al. 2005).

The sensitivity of CT for a systematic detection of bone metastases is poorly known. It is more sensitive than radiographs for lesion detection and provides information on the adjacent soft tissues (Bauerle and Semmler 2009). Comparison with MRI and PET shows a lower sensitivity of CT compared to these techniques (Yang et al. 2011; Sundaram and McGuire 1988). Moreover, as for radiographs and BS, CT can be falsely positive in the evaluation of response to therapy, due to the appearance of osteosclerotic areas in relation to the response to treatment within osteolytic or previously undetected lesions. This is frequently illustrated by the correlation of CT and PET findings before and after therapy of bone metastases (Fig. 3).

For these reasons, CT is not used as a primary tool for bone lesions monitoring. However, the technique is available in a significant proportion of cancer patients, as thoraco-abdomino-pelvic examinations are often repeated for visceral lesion detection and follow-up. These examinations provide a "free access" to bones, especially the spine and pelvis. This bone study can then be optimized by the use of adequate acquisition and reconstruction parameters (windows, kernels, slice thickness…). On these examinations, an increase in size of an osteolytic lesion, appearance of osteolysis in a previously sclerotic lesion and increase in the soft tissue extension of a bone lesion can be regarded as reliable signs of disease progression. Any other observation (lack of change, appearance of sclerosis, appearance of a new sclerotic areas…) should be considered more cautiously and should not be taken into account for valuable response evaluation (Figs. 3, 4) (Hamaoka et al. 2004).

In multiple myeloma, comparison of whole body CT (WBCT) to WBMRI for lesion screening has shown that WBCT was less sensitive to detect the bone involvement by the disease (Baur-Melnyk et al. 2008).

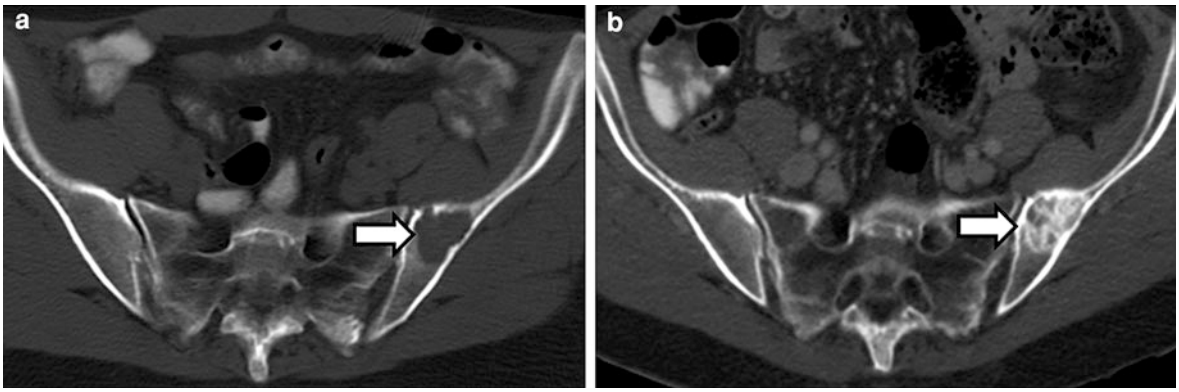

Fig. 4 CT follow-up of osteolytic metastasis. **a** Initial CT reveals lytic lesion within the posterior left iliac crest. **b** Follow-up after chemotherapy shows sclerosis of this lesion suggestive of response to the treatment

6 Positron Emission Tomography and PET-CT

PET provides metabolic—functional—information on the uptake of positron-emitting tracers by tissues. It enables a "whole body—all organ" screening. The combination of PET with CT and more recently with MRI on hybrid scanners combines the functional information provided by PET to the improved anatomic localization offered by CT (Hamaoka et al. 2004; Antoch et al. 2003). Under treatment, both PET and CT provide original and complementary information on the evolution of lesions: decrease in metabolic activity and increase in CT attenuation due to osteoblastic reaction are observed in responding lesions (Fig. 4) (Yang et al. 2011; Tateishi et al. 2008).

The most commonly used PET radiopharmaceutical, 18F-fluorodeoxyglucose (18FDG), is a non-specific tracer analog of glucose. It provides information on glucose metabolism and transport associated with several tumors, but also with some benign conditions. It enters the neoplastic cells by a membrane protein and is trapped within the cell once phosphorylated into FDG-6-phosphate. The technique allows qualitative whole body screening, showing often the primary lesion and its metastases to various organs (Fig. 5). Quantitative analysis is also obtained through the measurements of standardized uptake values (SUV), which reflect the tissue activity within a region of interest corrected for the injected activity and for the patients' body weight. Assessment of response is based on the follow-up of these qualitative and quantitative analyses.

18FDG-PET has proven to be a technique of choice for whole organ staging and follow-up of several cancers, especially lung, breast, head and neck neoplasms, melanoma, lymphoma (Tateishi et al. 2008; De Giorgi et al. 2010). However, the translation of PET to the daily practice of oncology as a tool of response assessment requires several precisions: the definition of cut-off quantitative changes for defining response/progression, time intervals for follow-up, and the optimal indications of CT as adjunct in PET-CT (dose, contrast…) (Shankar et al. 2006; Young et al. 1999; Suzuki et al. 2008).

FDG is a nonuniversal tracer. Several cancers and secondary lesions, especially prostate, neuroendocrine or some bronchial cancers, and osteoclerotic meta stases, show little affinity for this marker compared to other cancers and osteolytic lesions (Yang et al. 2011; Young et al. 1999; Shreve et al. 1996). Other tracers have been developed to target cancers with poor affinity for FDG, on the basis of other metabolic pathways. Their availability in clinical practice is less evident due to more difficult synthesis and shorter half-life. Among these, 11C/18F-choline and 11C-acetate raise much interest, especially in prostate cancer. Choline is transported into cells and trapped as a constituent of the membrane phospholipids. 18F-choline and 11C-choline have respective advantages and limitations. 18F-choline is excreted in the urine, which interferes with pelvic imaging. 11C-choline is better suited for pelvic imaging but interferes with upper abdomen imaging due to

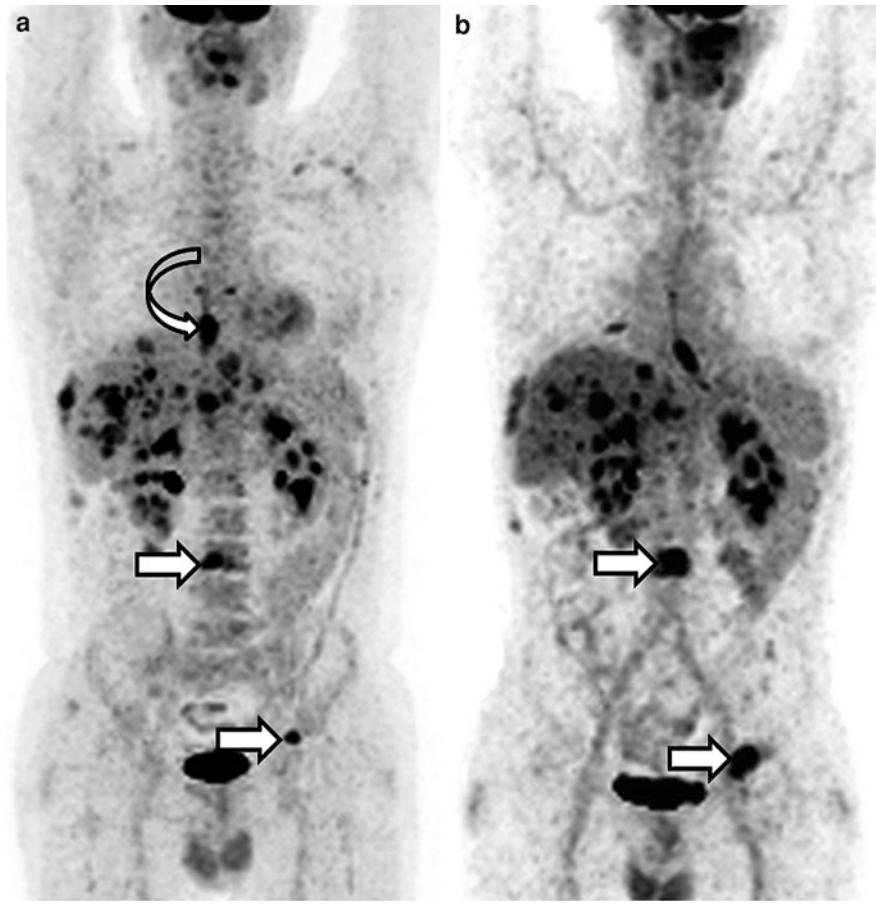

Fig. 5 FDG PET, staging and follow-up, in a patient with cancer of the oeso-gastric junction. **a** The technique not only shows the primary tumor (*curved arrow*), but also enables all organs screening: liver mets are evident, and bone mets are present in a right rib, in a lower lumbar vertebra and in the left iliac bone (*arrows*). **b** Six-month follow-up PET shows evident increase in size of the lumbar and iliac lesions, with heterogeneous behavior of the liver lesions

accumulation in the liver, kidneys, pancreas and spleen; moreover, its very short half-life limits its use to sites with cyclotrons (Langsteger et al. 2006). 11C-acetate also shows marked uptake in prostate cancer and has been shown to be more sensitive to detect prostate cancer than 18FDG PET; but there is limited information on bone metastases (Oyama et al. 2002). Another interesting tracer is 18F-fluoride, taken up by bone metastases in relation with their osteoblastic activity, incorporated as fluoroapatite at the bone surface where the turnover is the greatest, leading to conspicuous distinction between metastases and adjacent normal bone. The images resemble those obtained at BS, but with higher quality and higher spatial resolution, and the technique appears superior to BS for detecting both osteoblastic and osteolytic bone metastases (Even-Sapir et al. 2006).

Finally, additional radiopharmaceuticals are developed, targeting specific tumor receptors, especially in hormonal receptor-positive breast cancer and in neuroendocrine cancers.

7 Magnetic Resonance Imaging

Radiographs, BS and CT only detect neoplastic lesions to bone at a relatively late stage, weeks or months after the appearance of tumor cells within the bone marrow, since they rely on the activation of bone cells—osteoblasts and osteclasts—to become able to detect the tumor. MRI is sensitive to early changes in bone marrow that precede this osteoclastic/osteoblastic response of the bone matrix to tumor

infiltration, before bone trabeculae or cortices are affected by the disease (Vande Berg et al. 1998a, b).

The availability of the technique, its repeatability, the lack of irradiation and its ability to provide (almost) whole body evaluation contribute to promote MRI as a first line tool for the detection and characterization of many tumoral lesions involving the skeleton, and from there for the staging of cancers and evaluation of their response to treatment. Besides conventional anatomic sequences, advances in perfusion and diffusion imaging further refine the assessment of tumoral lesions during the (early) phases of therapy, providing the clinician with tools to evaluate the efficacy of treatments targeting bone lesions (Messiou et al. 2009).

7.1 Sequences

MRI contrast relies on the differences in T1 and T2 relaxation times between neoplastic lesions and their normal marrow environment. Metastatic infiltration of the bone marrow leads to a lengthened T1 relaxation time and signal loss, which contrasts with the surrounding high signal related to the fat content of the bone marrow (Vande Berg et al. 1998a).

T1-weighted images are the basis of bone marrow screening, due to their exquisite sensitivity to the alteration of the balance between fat and nonfat components of the bone marrow and to their universality, i.e. transposability for acquisition and reading from one center to the other, from one magnet to the other and, in the setting of assessment of treatment response, from one examination to the other. While these T1-weighted images are often sufficient for lesion detection and follow-up under treatment, especially in patients with poor (fatty) surrounding bone marrow in relation with age or treatment, most centers acquire additional T2 or T2-equivalent images (T2-weighted fat-suppressed or short tau inversion recovery (STIR) sequences) as part of the routine marrow screening and follow-up. Post-injection images and quantitative evaluation of marrow enhancement after contrast injection are only obtained when the distinction is not evident on conventional sequences between diffuse neoplastic infiltration and benign hyperplasia of the bone marrow or for the optimal definition of the extra osseous spread of tumors, for example within the spinal canal (Vande Berg et al. 2005; Baur et al. 1997). This injection of contrast material is also indicated when meningeal carcinomatosis is suspected.

7.2 Target Anatomic Areas

As hematologic cancers and metastases have a preferential tropism for red marrow containing skeletal areas, MRI studies will "focus" on these areas, for both lesion detection and follow-up. Screening of the whole spine in the sagittal plane and pelvis in the coronal plane covers about 90% of these skeletal areas and is considered sufficient by many authors, offering reproducibility, rapidity, with no or very little loss in diagnostic performance compared to whole body studies, since the vast majority of patients presenting lesions in the peripheral skeleton also present lesions within the central skeleton (Lecouvet et al. 2010; Russell et al. 1966). Of note, an MRI study limited to the spine appears insufficient, at least in multiple myeloma, for the marrow screening (Bauerle and Semmler 2009). However, whole body protocols with their increasing availability on MR magnets, with the improvement in their image resolution and shortening of acquisition time, along with the development whole body DWI (WBDWI) and "all organ" capabilities (cf. infra), are now being employed at many institutions (Schmidt et al. 2009; Moynagh et al. 2010).

7.3 Target Cancers

Screening of the skeleton for neoplastic lesions and evaluation of their response to therapy has major importance in "osteophilic" cancers (i.e. prostate, breast, kidney, thyroid, lung…) and in hematologic disorders involving bones (i.e. multiple myeloma and lymphoma).

As bone tumors have been considered "non measurable" for years, the use of MRI for the assessment of lesion response in patients who were previously treated "blinded" or based on the limited value of "skeletal related events", offers new perspectives and generates wide interest in many malignancies, especially in prostate and breast cancers, lymphoma and myeloma (Dreicer 1997).

For several of these cancers, other tools, especially 18FDG-PET scan as already mentioned, offer reliable

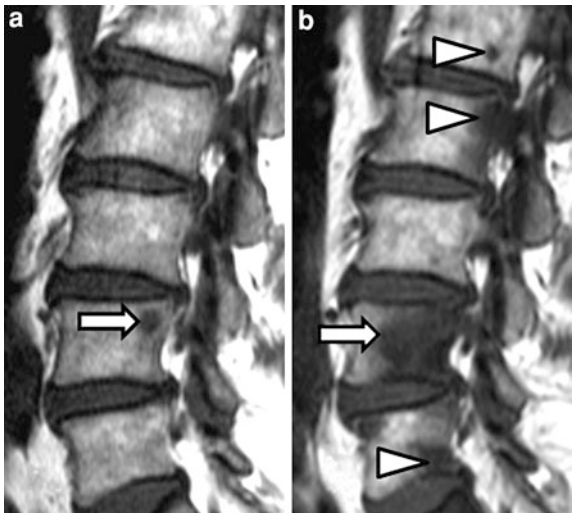

Fig. 6 Progressive metastatic disease at MRI: increase in the number and size of marrow lesions in a man with prostate cancer. **a** Sagittal T1-weighted MR image of the lumbar spine shows an isolated focus of low signal intensity within L4, corresponding to a metastasis (*arrow*). **b** Despite initiation of systemic therapy, 3-month follow-up MR image shows increase in the L4 lesion (*arrow*), and multiple new lesions (*arrowheads*), indicating disease progression

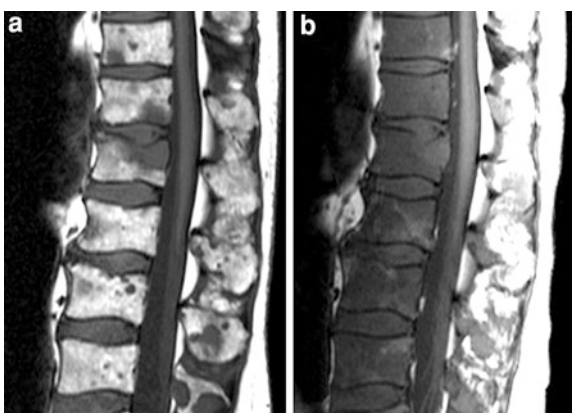

Fig. 7 Progressive metastatic disease: evolution from multifocal marrow lesions to diffuse neoplastic marrow infiltration in a man with prostate cancer. **a** Sagittal T1-weighted MR image of the lumbar spine shows multiple foci of low signal intensity within the vertebral bodies and posterior elements, corresponding to metastases. **b** Despite initiation of systemic therapy, 3-month follow-up MR image shows severe diffuse decrease of the marrow signal indicating progression of the neoplastic infiltration of the bone marrow

all organ screening and response evaluation. This technique is very efficient in lung cancer and lymphoma, for example. The comparison between PET

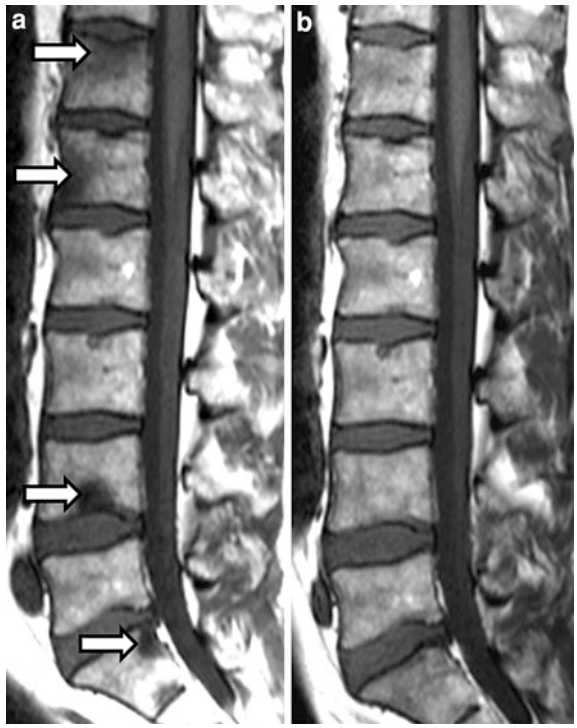

Fig. 8 Complete response: evolution from multifocal marrow lesions to normal marrow appearance in a woman with breast cancer. **a** Initial sagittal T1-weighted MR image of the lumbar spine shows multiple foci of low signal intensity, corresponding to metastases (*arrows*). **b** After 3-month systemic therapy, follow-up image shows complete disappearance of the lesions and return to normal homogeneous high signal intensity of the bone marrow

and WBMRI in terms of diagnostic performance, and also in terms of costs, has to be assessed (Ghanem et al. 2005; Antoch et al. 2003; Schmidt et al. 2007).

7.4 Qualitative (Morphologic) Analysis of Bone Marrow Involvement and of Tumor Response

The patterns of marrow involvement in metastatic disease to bone and in hematologic malignancies have been widely described (Vande Berg et al. 1998a, b). Contrasting with the homogeneous relatively high signal intensity of the normal bone marrow on T1-weighted images and its low signal on STIR or PD fat saturated images, the neoplastic involvement of the marrow will present either a focal appearance (low/intermediate to high signal intensity foci on T1/STIR or PD-fs images) or a diffuse appearance (diffuse low/

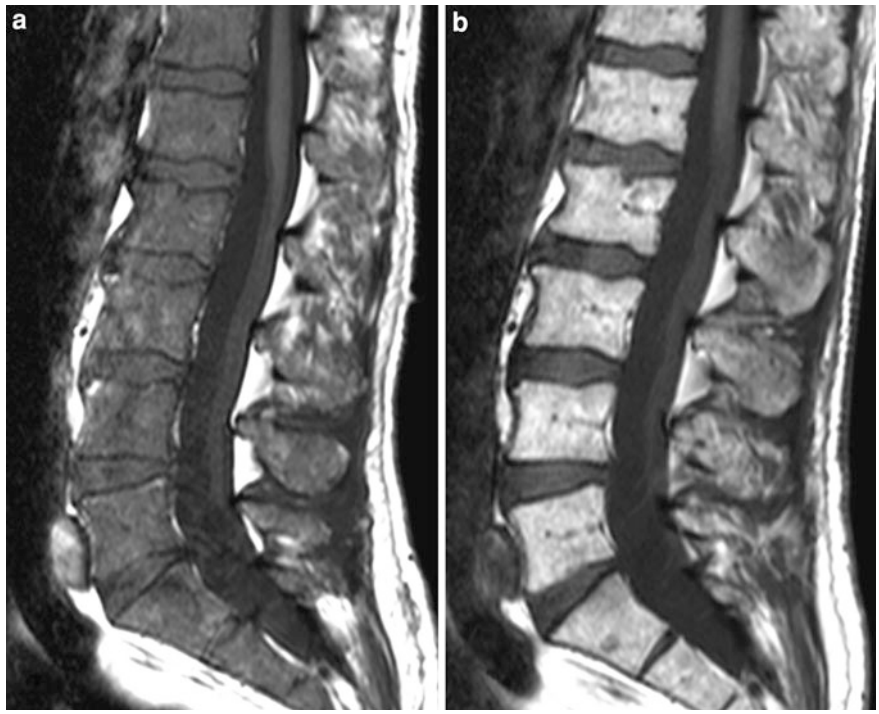

Fig. 9 Complete MRI response: evolution from diffuse marrow infiltration to return to normal marrow appearance in a man with myeloma. **a** Initial sagittal T1-weighted MR image of the lumbar spine shows diffuse decrease of the marrow signal, identical to that of disks, indicating diffuse neoplastic infiltration. **b** After 6-month systemic therapy, follow-up MR image shows complete return to homogeneous high signal intensity of the bone marrow (complete remission was confirmed by bone marrow biopsy and seric tests)

intermediate to high signal intensity of the marrow, which becomes lower than disk or muscle signal intensity on T1-weighted images). Besides these focal and diffuse patterns, a less common "salt and pepper" pattern, characterized by multiple tiny foci of abnormal marrow signal, is reported, especially in hematologic malignancies (Baur-Melnyk et al. 2008; Vande Berg et al. 1998a).

The follow-up of patients with neoplastic bone involvement after treatment may show evolutions in these patterns. Some of these changes are with no ambiguity indicative either of disease progression or on the contrary of response to treatment. Evolution from a normal bone marrow appearance to a focal metastatic pattern or to diffuse marrow signal alteration, increase in the number and/or size of metastatic foci, evolution from focal to diffuse neoplastic infiltration will be indicative of progressive disease (Fig. 6, 7). Disappearance of focal lesions, decrease in their number and/or size and return from focal or diffuse marrow alterations to a normal marrow appearance are indicative of response to treatment (Fig. 8, 9). The complete disappearance of lesions may indicate "imaging" remission, which does not necessarily correlate with complete remission at the microscopic level.

Perfect stability in size and appearance of the marrow abnormalities after treatment should be interpreted cautiously: residual lesions may represent responsive, controlled, but still active disease or on the contrary, "cured" disease with persistence of "scar" tissue. Whether contrast material injection, study of perfusion or diffusion parameters will help or not in this difficult differential diagnosis remains uncertain. Some lesions showing evident decrease in their contrast enhancement after treatment have shown residual viable tumor cells at histology (Lecouvet et al. 1998a).

Relapse is characterized by the reappearance of one or several new lesions in a bone marrow that had shown previous return to normal appearance after therapy; sometimes it may also take the appearance of progression of a lesion that had previously shown size regression under treatment or was stabilized by this treatment.

A pitfall may be encountered when marrow stimulating factors are used in association with chemotherapy. This treatment may indeed lead to diffuse alteration of the bone marrow signal, with decrease of its signal intensity on T1-weighted images, due to marrow hyperplasia, which may be confusing for progression to diffuse neoplastic infiltration (Vande Berg et al. 2005; Ryan et al. 1995) (Fig. 10). The study

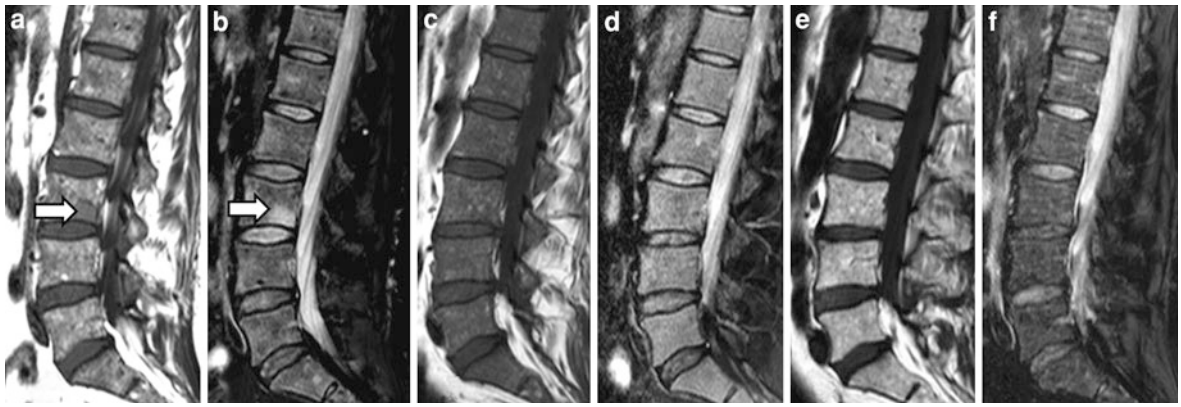

Fig. 10 False progression to diffuse marrow infiltration due to the use of hematopoietic growth factors in a treated multiple myeloma patient. **a**, **b** Pre-treatment T1- (**a**) and PD fat saturated (**b**) sagittal MRI of the lumbar spine show heterogeneous marrow signal with focus of marrow replacement in L3 (*arrow* in a and b). (**c**, **d**) After myeloablative treatment and intensive use of growth factors for stem cell mobilization before marrow transplantation, follow-up MR images show diffuse decrease of the marrow signal which becomes close to that of disks on T1 images of the spine (**c**) and discrete signal increase on PD fat saturated images (**d**). Contemporary bone marrow biopsy performed within the iliac crest revealed diffuse benign marrow hyperplasia. (**e**, **f**) Two-month follow-up MRI shows return to a normal homogeneous appearance of the bone marrow on all sequences

of marrow enhancement after contrast material injection and perfusion parameters enable the distinction between these conditions, as benign hyperplasia shows only limited enhancement compared to diffuse neoplastic infiltration (Baur et al. 1997).

Of note, metastatic cancer to bone may be a heterogeneous disease, with sometimes variable behavior among lesions under treatment, some of them showing obvious signs of response, while others show progression, suggesting appearance of resistance to treatment in some metastatic foci (Fig. 11). This observation underlines the need for extensive skeletal surveys, to avoid wrong conclusions (for instance, response) made on the basis of the follow-up of a limited number of lesions; this could advocate the use of WBMRI for lesion follow-up in multifocal skeletal involvement.

7.5 Particular Morphologic Aspects of Lesion Response

The response of focal marrow lesions to therapy may be characterized, along with their reduction in size, by the appearance of a peripheral halo of fatty marrow, with characteristic high signal intensity on T1-weighted images (Fig. 12). This "fatty halo sign" is indicative of lesion response and parallels the observation of the appearance of fat within "responsive" or "healing" nonneoplastic conditions such as benign vertebral compression fractures, spondylodiscitis or degenerative disk disease. In these conditions, the transition from "edema-like" marrow infiltration to "fat-like" signal also indicates stabilization or healing.

Contrasting with this "fatty" halo, a "cellular" halo, may be observed at the periphery of neoplastic lesions, consisting in a faint border with a low signal on T1 and high signal intensity on STIR/PD-fs images, which is interpreted as indicative of an "active" or "aggressive" tumoral lesion (Hwang and Panicek 2007). The disappearance of this halo at the periphery of treated lesions might be an early indicator of response.

Lesion response sometimes does not take the appearance of shrinking, but rather of progressive fading of the marrow signal abnormalities and return to normal marrow signal intensity within the lesions; whether this evolution is more typical for some types of treatments (cystostatic) remains to be established.

7.6 Ancillary Indicators of Response/ Progression

The occurrence of a pathologic fracture, due to focal bone weakening by a neoplastic lesion, and progression or appearance of soft tissue extension (for example

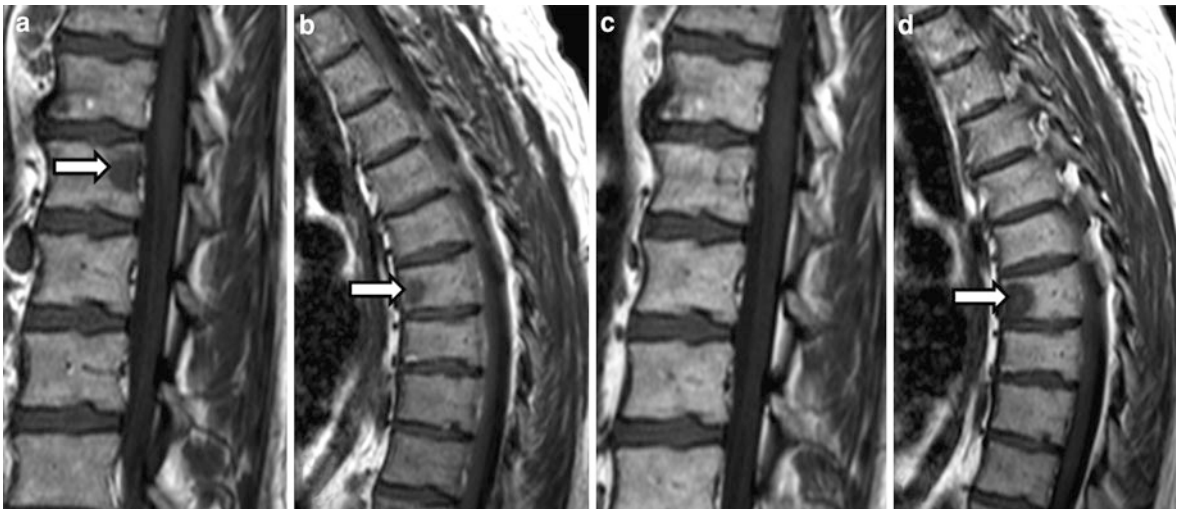

Fig. 11 Illustration of the potential asynchronic evolution of bone metastases. **a**, **b** Lumbar (**a**) and thoracic (**b**) sagittal T1-weighted MR images show two low signal intensity lesions corresponding to metastases (*arrows*). (**c**, **d**) After 3 months of systemic therapy, the lumbar lesion shows complete disappearance, whereas the thoracic lesion shows evident increase in size (*arrow* in **d**)

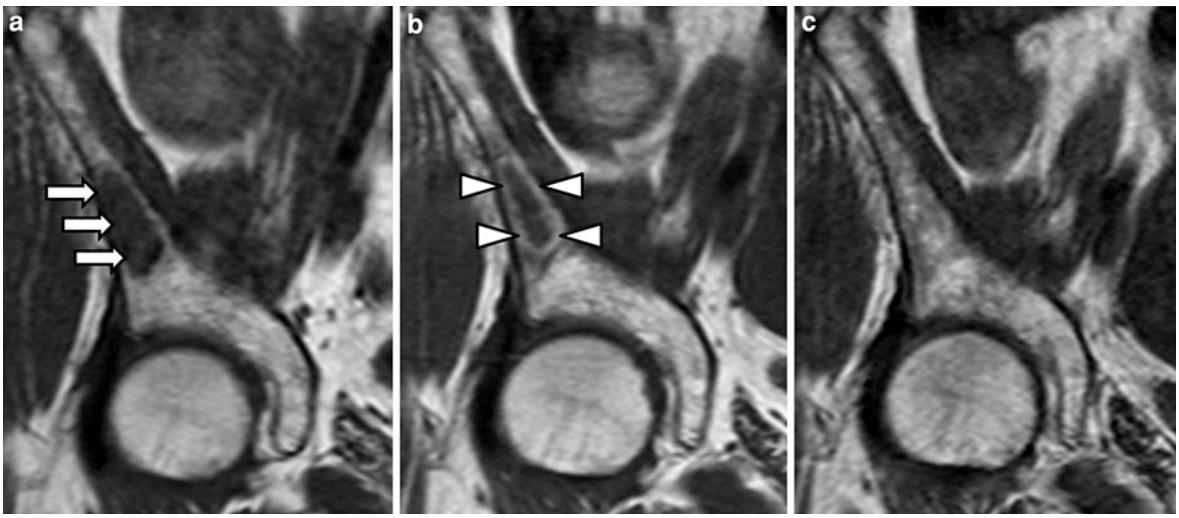

Fig. 12 Follow-up of neoplastic lesion during treatment: appearance of a peripheral fatty halo in a responding lesion. (**a**) Initial coronal T1-weighted MR image of the pelvis shows low signal intensity lesion within right iliac bone typical for a metastasis (*arrows*). (**b**) After 3-month systemic therapy, follow-up image shows the appearance of peripheral halo of high signal intensity, corresponding to fat surrounding the "shrinking" lesion (*arrowheads*). (**c**) Two-year follow-up shows complete disappearance of the lesion, with reappearance of normal marrow within the lesion

epidural) from a marrow lesion, are obvious signs of disease progression. Of note, benign osteoporotic fractures may occur during the course of the disease, which could be regarded as signs of disease progression on the basis of clinical records or conventional radiographs, but for which MRI shows the benign origin, sometimes contrasting with concurrent signs of response in neoplastic lesions. This discordance illustrates how "skeletal related events" are sometimes falsely indicative of progressive disease (Fig. 13).

The importance of the evaluation of soft tissue extension from bone lesions must be emphasized, especially in the spine environment. The presence of paraspinal or epidural infiltration may justify careful

Fig. 13 "Discordance" between MRI and clinical evaluation of response: appearance of a new vertebral fracture despite evident signs of response in a patient with metastatic breast cancer. **a** Initial sagittal T1-weighted MR image of the lumbar spine shows multiple foci of low signal intensity, corresponding to metastases. **b** After 3-month systemic therapy, follow-up image shows frank decrease in the size and number of neoplastic lesions, with increase in the marrow signal intensity. A new benign (osteoporotic) vertebral fracture is observed in L1 (*arrows* in b). This new "skeletal event" would represent evolutive disease in the absence of MRI monitoring

MR imaging follow-up if threatening or impinging on the spinal cord or nerve roots (Figs. 14, 15). Progression or appearance of soft tissue extension should be regarded as a sign of disease progression, sometimes more evident than changes observed within the originating bone lesions. Failure to regress under therapy may prompt the indication of surgical decompression of epidural extension (Fig. 14). In myeloma and lymphoma, the response of this tumoral extension to systemic or regional (radiation) therapy is often spectacular.

7.7 Quantitative Criteria

Several approaches are proposed to quantify the efficacy of treatment on bone lesions, inspired by tools used to evaluate the response to treatment using imaging in primary or secondary soft tissue tumors. These tools are mainly based on the follow-up of lesion size, and they use several response categories (progressive disease, complete response, partial response, stable disease) (RECIST). The evaluation of tumor burden provided by these various measurement tools and its follow-up during therapy show promising correlation with other imaging (soft tissue metastasis quantification) indices of tumor response to therapy and with the clinical and follow-up evaluation of treatment response in breast, prostate and other cancers (Brown et al. 1998; Ciray et al. 2001; Tombal et al. 2005). This offers the perspective to increase the number of patients (i.e. those with bone metastatic disease) in whom response to usual isolated treatments or to new drugs may be evaluated.

7.8 Diffusion-Weighted Imaging

The use of morphologic and size criteria for the assessment of the response of neoplastic lesions to therapy is facing limitations, for bone marrow MRI like for other techniques and other organs, mainly due to the difficult interpretation of lesion persistence after therapy and to the advent of new drugs with new effects, i.e., cytostatic therapies, which are known to have no, limited or delayed impact on lesion size despite histologic efficacy (Padhani and Koh 2011).

Without going into details of underlying physics and principles, DWI provides a measure of the mobility of water molecules in tissues (Bammer 2003). Though permanent, this motion (induced by the thermal agitation of the molecules) is restricted by several physiological barriers. Tissues with a higher cellularity, hence with higher proportions of membranes, intracellular organelles or restricted free extracellular space, demonstrate impeded water diffusibility compared to normal surrounding tissues, explaining the ability of DWI to detect tumoral conditions with increased cellular density.

DWI provides both morphologic (qualitative) as well as functional (quantitative) information on tumoral lesions. Reconstructed MIP or MPR images of DWI, covering the whole body or limited to the central skeleton, show tumoral foci with a high signal intensity on high b-value images, providing easy "at a glance" qualitative evaluation of the tumor burden and driving the attention to areas of difficult analysis on anatomic sequences. Comparison of DWI to skeletal scintigraphy or to PET (choline) for bone metastases detection in osteophilic cancers shows equivalent or superior

Fig. 14 Progression of bone and soft tissue extension in metastases from colon cancer: use of MRI to evaluate the response. **a**, **b** Initial sagittal (**a**) and transverse (**b**) T1-weighted MR images of the thoracic spine show multiple foci of low signal intensity, corresponding to metastases (*arrows* in **a**). Evident epidural extension is seen (*arrowheads* in **a** and **b**). Rib involvement with soft tissue extension is evident (*). (**c**, **d**) After 3 weeks of systemic therapy, corresponding follow-up images show increase in size of the bone metastases (*arrows* in **c**) and evident increase of the epidural extension and mass effect on the spinal cord (*arrowheads* in **c** and **d**) (indication of surgical decompression). Rib involvement with soft tissue extension also shows evident progression (*)

diagnostic value of DWI-MRI (Luboldt et al. 2008; Lecouvet et al. 2009; Gutzeit et al. 2010). The technique also shows great promises for response assessment. DWI is able to detect changes in water diffusion that occur after therapy as a result of changes in cellular density and loss of membrane integrity (Charles-Edwards and deSouza 2006; Padhani 2011). The impeded water mobility observed in tumoral tissue will decrease or disappear in relation with the loss of cellular integrity in response to treatment, for example due to the occurrence of necrosis (Charles-Edwards and deSouza 2006; Khoo et al. 2011; Koh et al. 2007). Comparison of two consecutive examinations obtained in a treated patient provides a rapid and generally non ambiguous evaluation of the disease response or progression under therapy (Fig. 16). Quantitative assessment is provided by the measurement of an apparent diffusion coefficient (ADC, units 10^{-3} mm^2/s) calculated from the diffusional signal attenuation following the application of motion sensitizing gradients. Generally, a decrease in ADC values due to the presence of a tumoral focus parallels the observation of a bright signal on high

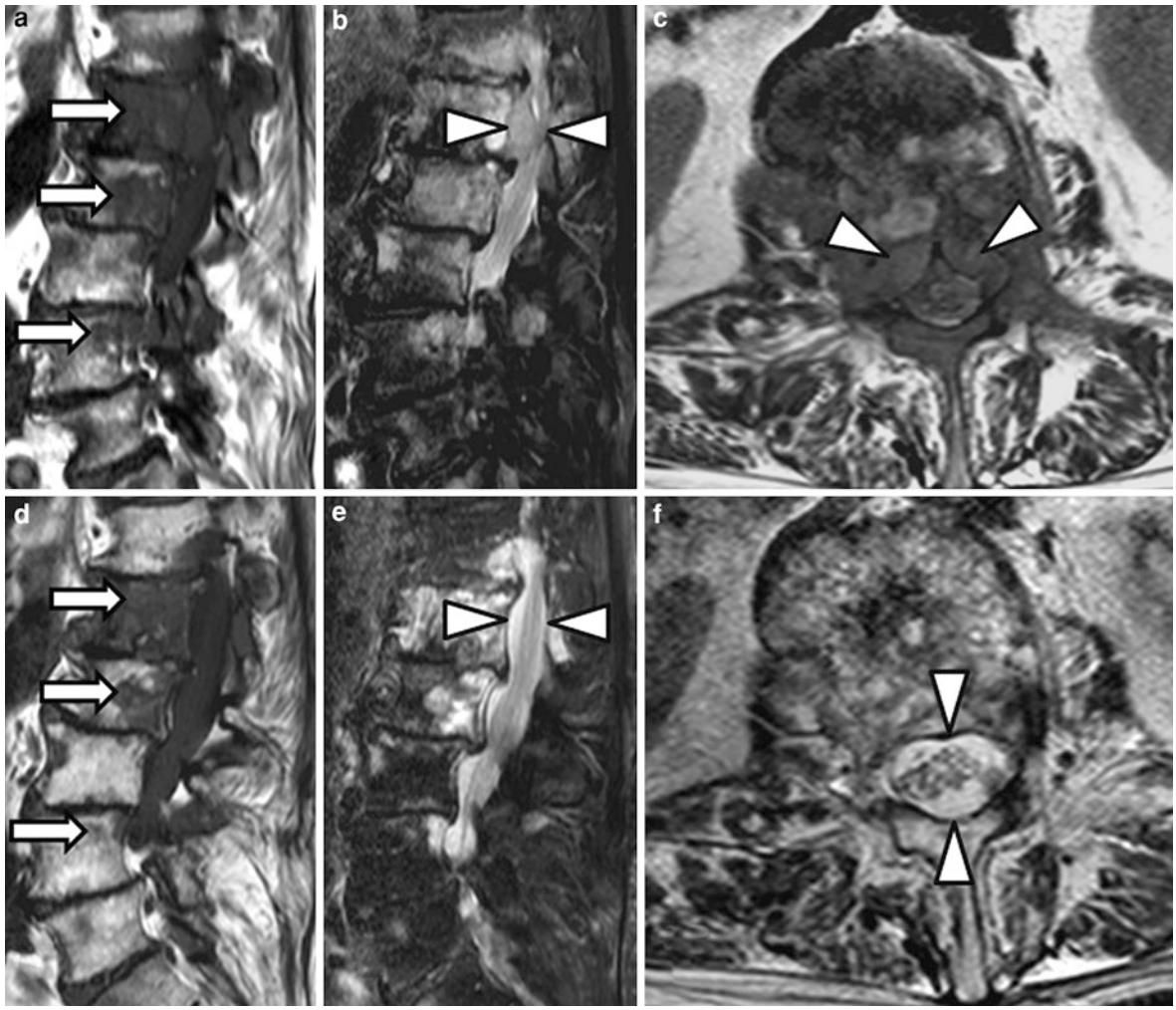

Fig. 15 Demonstration of response of soft tissue extension: lymphoma with multiple bone lesions and epidural extension: use of MRI to monitor the early response of epidural soft tissue extension (absence of response would lead to indication of surgical decompression). (**a**, **b**, **c**) Initial sagittal T1 and PD fat saturated (**b**) MR images of the lumbar spine show multiple foci of low signal intensity, corresponding to metastases (*arrows* in **a**). Evident epidural extension is seen, impinging on the cauda equina (*arrowheads* in **b**). Transverse T2-weighted MR image shows the retropulsion of the posterior longitudinal ligament by this soft tissue extension (*arrowheads* in **c**). (**d**, **e**, **f**) After 2-weeks of radiation and systemic therapy, corresponding follow-up T1 image shows decrease in size of the bone lesions (*arrows* in **d**) and increase in the marrow signal in relation to irradiation; T2-weighted MR images show complete disappearance of the epidural extension and mass effect on the nerve roots (*arrowheads* in **e** and **f**)

b-values DW images, in relation to the increased cellularity and increased water content in the tumor. Follow-up of treated lesions show concurrent decrease of lesion signal on high b-values MR images and increase in ADC values (Byun et al. 2002). This decrease in ADC values in tumors compared to surrounding tissues can be monitored over time after chemotherapy (Byun et al. 2002). DWI has been shown able to detect ADC increase within prostate cancer metastases treated with antiandrogen therapy as early as one month after treatment initiation (Gutzeit et al. 2010; Koh et al. 2007; Reischauer et al. 2010). The effectiveness of ADC monitoring to predict the response of bone metastases to therapy is however controversial (Messiou et al. 2011). The interpretation of changes in ADC values is indeed complex, mainly due to tumor and response heterogeneity. Post-treatment necrosis may sometimes be characterized by the

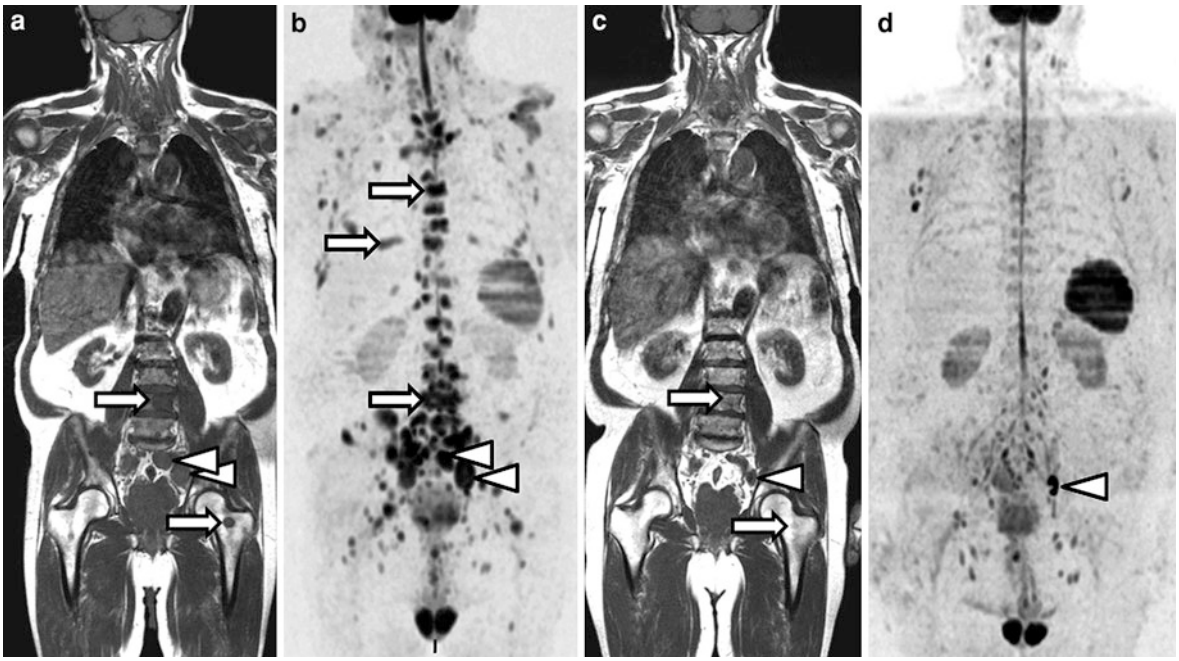

Fig. 16 Follow-up of metastatic prostate cancer during treatment using whole-body MRI: disappearance of bone and lymph node lesions. (**a**, **b**) Initial coronal T1- and diffusion-weighted MR images of the whole body show lesions typical for bone metastases (*arrows*) and concurrent pelvic lymph nodes (*arrowheads*). (**c**, **d**) After 3-month hormonotherapy, follow-up images show the disappearance of bone lesions (*arrows*) and only one small size residual lymph node (*arrowhead*)

observation of persisting high signal foci on DWI images, but with increased ADC values due to loss of membranes; this is called the "T2 shine through effect". Other pitfalls in the visual analysis of high b-values DW images exist and must be known. Since DWI not only reflects cellular load but also water content of tissues, benign conditions such as degenerative joint diseases, fractures, post-radiation changes or benign tumors (angiomas) may present a high signal intensity on DWI images. The technique may also present false negative findings, mainly in very sclerotic or calcified metastases. These pitfalls underline the need for a systematic correlation of DW images with the morphologic appearance of the lesions on conventional MR sequences among which T1-weighted images are most likely the more helpful (Lecouvet et al. 2009; Koh et al. 2007; Komori et al. 2007). Newer analysis methods (called ADC parametric response map or functional diffusion map) take into account spatial information and tumor heterogeneity. They are based on careful voxel-by-voxel follow-up of treatment induced changes and evaluation of the proportion of tumor tissue in which significant changes occur (Reischauer et al. 2010). These approaches seem to be able to detect very early changes – increase in ADC – after treatment initiation (Lee et al. 2007).

Finally, one must remember that the relationship between the ADC and the actual diffusion of water molecules in the tissues of interest is highly complex and influenced by DWI sequence parameterization. Though single-shot echo planar imaging (SS-EPI) is the most common technique of acquisition, multi-shot EPI (MS-EPI), single-shot fast spin echo (SS-FSE) or steady state free precession (SSFP) can also used in DWI (Khoo et al. 2011). Diffusion can be hypothesized isotropic or anisotropic, thus modifying the orientation and the number of diffusions gradients to be used. The diffusional signal decay can be modeled using a mono-exponential (most often), multi-exponential or stretched-type function. The interval and number of b-values used impact ADC measurements as well as the delineation of the tumor from normal or necrotic tissues. Theoretically, high b-values are required to cancel the blood flow contribution (i.e. perfusion) to the water molecules mobility, in order to study the true diffusional motion. These issues are the subject of many studies.

7.9 Dynamic Contrast-Enhanced MRI

DCE—or perfusion—MRI provides information on tumor perfusion and permeability of vessels. This technique has been proven useful for the early monitoring of the response to various anticancer treatments, especially those targeting tumoral angiogenesis (Montemurro et al. 2004; Bauerle et al. 2010).

Perfusion uses repeated imaging (i.e. a dynamic sequence) to track the entrance of a diffusible tracer into a tissue over time. When the dynamic sequence is T2*-weighted, perfusion is based on susceptibility contrast (DSC-MRI). DSC-MRI is mainly used in brain imaging where tracer extravasation is expected to be limited due to the blood brain barrier. When the sequence is T1-weighted, a contrast-enhanced imaging (DCE-MRI) is achieved. DCE-MRI is the standard method used in cancers outside the brain and in the particular setting of bone marrow cancers, where tracer extravasation is important due to a rupture (or a hyperpermeability) of the endothelial barrier.

The principle of the technique may be summarized as follows. Shortly after its injection, the tracer begins to circulate through the body and diffuses over time into the extravascular extracellular space, inducing changes in the signal intensity. These signal changes over time are studied in the tissues of interest, either qualitatively (study of enhancement patterns), semi-quantitatively (study of the maximum up-slope, area under the curve, time to peak or wash-out slope…) or quantitatively (study of physiological parameters such as blood flow, blood volume, interstitial volume or permeability-surface area product derived from a kinetic model fitted to the curve). Quantitative models provide parameters independent from the MR acquisition and interesting simplified physiological information reflecting the actual mechanisms of transport in tissues.

The usefulness of DCE-MRI in normal and pathological vertebral bone marrow, in various benign and malignant musculoskeletal lesions and its prognostic potential in multiple myeloma has been demonstrated (Hawighorst et al. 1999; Biffar et al. 2010; Hillengass et al. 2007). The evaluation of DCE-MRI in early clinical trials has shown that the technique provides useful information on tumor biology and response to treatment (O'Connor et al. 2007).

DCE-MRI presents certain practical, as well as theoretical, limitations. The first limitation of DCE-MRI remains the need for an intravenous injection of a paramagnetic contrast agent. Since quantitative DCE-MRI relies on signal intensity conversion into a measure of tracer concentration, the relationships between concentration and relaxation time T1 on one hand, and between T1 and signal intensity on the other hand, have to be accurately determined. It is known that inter-compartmental water exchange kinetics and B1 field inhomogeneities have a critical influence on the determination of these relationships (Yankeelov et al. 2003; Buckley et al. 2008; Parker et al. 2001). Moreover, for the determination of quantitative parameters, an arterial input function (AIF) (providing the knowledge of tracer concentration in the blood plasma) needs to be measured, which is more difficult to achieve in the coronal or sagittal planes, due to partial volume and inflow effects. As a result, analysis of a complete anatomic vertebra is often semi-quantitative (Hillengass et al. 2007). Alternative methods eliminating the need for a direct AIF measurement, such as the reference region model, are investigated (Yankeelov et al. 2003). As high temporal resolution is privileged for kinetic modeling, DCE images present limited spatial resolution, SNR and anatomic coverage (Kershaw and Cheng 2010). The estimation of the tumor perfusion and permeability may differ according to the kinetic model. Although the extended Tofts model is commonly used (because of its simple implementation), more sophisticated models can be discussed (Tofts et al. 1999; St Lawrence et al. 1998; Donaldson et al. 2010)

8 Multiple Myeloma

The radiographic skeletal survey is still performed as a key point in disease staging, as the detection of lytic lesions directly leads to categorization of the disease as advanced and requiring treatment (Durie and Salmon 1975). Since MRI is superior to radiography for the detection of bone marrow infiltration by plasma cells, an alternative "Durie and Salmon +"

staging system has been proposed, integrating the results of MRI (Durie 2006).

Bone marrow presents the same alterations at MRI as those described in other malignancies; a normal bone marrow appearance, focal lesions, diffuse infiltration or more discrete "salt and pepper" changes may be observed (Lecouvet et al.1998b). The definitive role of MRI for staging the disease remains, however, controversial. Axial skeleton or WBMRI is recommended in patients with myeloma who present with normal conventional radiographs and should be performed as part of staging in all patients with a solitary plasmacytoma of bone (Hillengass et al. 2010; Moulopoulos et al. 1993). In these settings, the observation of marrow lesions is correlated with a higher risk of disease progression and participates to the indication of systemic therapy.

MRI has been evaluated for the assessment of the response of MM to systemic treatment. The morphologic changes indicative of response include reduction in focal lesion size, return from a focal or diffuse pattern of neoplastic marrow involvement to a normal bone marrow appearance, decrease in diffuse marrow enhancement, and in focal lesion enhancement after contrast injection, with sometimes a residual peripheral enhancement halo (Moulopoulos et al. 1994). The lack of enhancement within a treated lesion should be considered carefully, as residual viable myeloma cells may be observed in this setting (Baur-Melnyk et al. 2005; Lecouvet et al. 1998a; Lecouvet et al. 2001). The complete disappearance of focal lesions with return to a completely normal marrow signal may be a very slow process (Hanrahan et al. 2010).

The role of imaging in patient follow-up and response assessment in MM remains controversial. Since lytic lesions show no or very delayed healing, the radiographic skeletal survey has no role in monitoring the response to treatment (Smith et al. 2006). Post-treatment monitoring with MRI is not currently systematic in MM, but several indications are established. MRI is the modality of choice in patients with focal symptoms, especially if a spinal complication is suspected, in non secretory myeloma to assess the treatment response, in cases suspect for relapse especially after high dose cytotoxic therapy and bone marrow transplantation, or after treatment of plasmocytoma. In this situation, MRI will substantiate a suspicion of relapse, and localize a target lesion that is then often biopsied using CT guidance to confirm this relapse.

Both DCE-MRI and DWI are proposed as potential tools for the early evaluation of treatment response in patients with MM. Early decrease in enhancement and increase in ADC values have shown positive correlation with response of the disease (Horger et al. 2011; Li et al. 2010). Although PET-CT can provide complementary information to MRI, its use in staging and follow-up of MM requires further evaluation before considering its role in clinical practice (Terpos et al. 2011).

9 Lymphoma

PET and, better, PET-CT, are the imaging methods of choice for "whole body—all organ" staging and for the evaluation of disease response after treatment, at least in Hodgkin lymphomas (HL) and aggressive non Hodgkin lymphomas (NHL), especially diffuse large B-cell NHL (DLBCL) (Juweid et al. 2007). In these indications, PET-CT outperforms anatomic imaging modalities. The value of PET relies on its ability to distinguish between viable tumor and necrosis or fibrosis in residual masses often present after treatment in patients without any other clinical or biochemical evidence of disease.

At morphologic analysis, evident increased (multi) focal bone marrow uptake is considered positive for lymphoma. Diffusely increased bone marrow uptake, after treatment, should be interpreted more cautiously, as it may be due to post-therapy marrow hyperplasia, spontaneous or "iatrogenic" (use of marrow stimulating factors), which may be confusing for diffuse lymphomatous marrow involvement (Messiou et al. 2009; Chhabra et al. 2006; Sugawara et al. 1998). However, a negative PET in the bone marrow does not completely rule out bone marrow involvement. Bone marrow biopsy, therefore, remains the standard procedure for assessment of bone marrow, although the use of MRI and of PET-MRI will probably raise interest in this setting (Messiou et al. 2009).

Besides this established value of PET-CT, WBMRI and WBDWI are emerging as an alternative diagnostic method for the staging of lymphomas,

and for the evaluation of their response to therapy, with reliable results (Abdulqadhr et al. 2011; Wu et al. 2011; Gu et al. 2011; Kwee et al. 2010; Vermoolen et al. 2011). An important advantage of MRI is the absence of irradiation, which is particularly interesting in a disease that involves young patients and requires repeated imaging follow-up.

References

Abdulqadhr G, Molin D, Astrom G, Suurkula M, Johansson L, Hagberg H, Ahlstrom H (2011) Whole-body diffusion-weighted imaging compared with FDG-PET/CT in staging of lymphoma patients. Acta Radiol 52:173–180. doi:10.1258/ar.2010.100246

Antoch G, Vogt FM, Freudenberg LS, Nazaradeh F, Goehde SC, Barkhausen J, Dahmen G, Bockisch A, Debatin JF, Ruehm SG (2003) Whole-body dual-modality PET/CT and whole-body MRI for tumor staging in oncology. JAMA 290:3199–3206

Avrahami E, Tadmor R, Dally O, Hadar H (1989) Early MR demonstration of spinal metastases in patients with normal radiographs and CT and radionuclide bone scans. J Comput Assist Tomogr 13:598–602

Balliu E, Boada M, Pelaez I, Vilanova JC, Barcelo-Vidal C, Rubio A, Galofre P, Castro A, Pedraza S (2010) Comparative study of whole-body MRI and bone scintigraphy for the detection of bone metastases. Clin Radiol 65:989–996

Bammer R (2003) Basic principles of diffusion-weighted imaging. Eur J Radiol 45:169–184

Bauerle T, Semmler W (2009) Imaging response to systemic therapy for bone metastases. Eur Radiol 19:2495–2507. doi:10.1007/s00330-009-1443-1

Bauerle T, Merz M, Komljenovic D, Zwick S, Semmler W (2010) Drug-induced vessel remodeling in bone metastases as assessed by dynamic contrast enhanced magnetic resonance imaging and vessel size imaging: a longitudinal in vivo study. Clini Cancer Res 16:3215–3225. doi:10.1158/1078-0432.CCR-09-2932

Baur A, Stabler A, Bartl R, Lamerz R, Scheidler J, Reiser M (1997) MRI gadolinium enhancement of bone marrow: age-related changes in normals and in diffuse neoplastic infiltration. Skeletal Radiol 26:414–418

Baur-Melnyk A, Buhmann S, Durr HR, Reiser M (2005) Role of MRI for the diagnosis and prognosis of multiple myeloma. Eur J Radiol 55:56–63. doi:10.1016/j.ejrad.2005.01.017

Baur-Melnyk A, Buhmann S, Becker C, Schoenberg SO, Lang N, Bartl R, Reiser MF (2008) Whole-body MRI versus whole-body MDCT for staging of multiple myeloma. Am J Roentgenol 190:1097–1104. doi:10.2214/AJR.07.2635

Biffar A, Sourbron S, Schmidt G, Ingrisch M, Dietrich O, Reiser MF, Baur-Melnyk A (2010) Measurement of perfusion and permeability from dynamic contrast-enhanced MRI in normal and pathological vertebral bone marrow. Magn Reson Med 64:115–124. doi:10.1002/mrm.22415

Brown AL, Middleton G, MacVicar AD, Husband JE (1998) T1-weighted magnetic resonance imaging in breast cancer vertebral metastases: changes on treatment and correlation with response to therapy. Clin Radiol 53:493–501

Buckley DL, LE Kershaw, Stanisz GJ (2008) Cellular-interstitial water exchange and its effect on the determination of contrast agent concentration in vivo: dynamic contrast-enhanced MRI of human internal obturator muscle. Magn Reson Med 60:1011–1019. doi:10.1002/mrm.21748

Byun WM, Shin SO, Chang Y, Lee SJ, Finsterbusch J, Frahm J (2002) Diffusion-weighted MR imaging of metastatic disease of the spine: assessment of response to therapy. Am J Neuroradiol 23:906–912

Charles-Edwards EM, deSouza NM (2006) Diffusion-weighted magnetic resonance imaging and its application to cancer. Cancer Imaging 6:135–143. doi:10.1102/1470-7330.2006.0021

Chhabra A, Batra K, Makler PT, Makler PT, Jr (2006) Obscured bone metastases after administration of hematopoietic factor on FDG-PET. Clin Nucl Med 31:328–330. doi:10.1097/01.rlu.0000218575.91735.5f

Ciray I, Astrom G, Andreasson I, Edekling T, Hansen J, Bergh J, Ahlstrom H (2000) Evaluation of new sclerotic bone metastases in breast cancer patients during treatment. Acta Radiol 41:178–182

Ciray I, Lindman H, Astrom KG, Bergh J, Ahlstrom KH (2001) Early response of breast cancer bone metastases to chemotherapy evaluated with MR imaging. Acta Radiol 42:198–206

Condon BR, Buchanan R, Garvie NW, Ackery DM, Fleming J, Taylor D, Hawkes D, Goddard BA (1981) Assessment of progression of secondary bone lesions following cancer of the breast or prostate using serial radionuclide imaging. Br J Radiol 54:18–23

Coombes RC, Dady P, Parsons C, McCready VR, Ford HT, Gazet JC, Powles TJ (1983) Assessment of response of bone metastases to systemic treatment in patients with breast cancer. Cancer 52:610–614

Daldrup-Link HE, Franzius C, Link TM, Laukamp D, Sciuk J, Jurgens H, Schober O, Rummeny EJ (2001) Whole-body MR imaging for detection of bone metastases in children and young adults: comparison with skeletal scintigraphy and FDG PET. Am J Roentgenol 177:229–236

De Giorgi U, Mego M, Rohren EM, Liu P, Handy BC, Reuben JM, Macapinlac HA, Hortobagyi GN, Cristofanilli M, Ueno NT (2010) 18F-FDG PET/CT findings and circulating tumor cell counts in the monitoring of systemic therapies for bone metastases from breast cancer. J Nucl Med 51:1213–1218. doi:10.2967/jnumed.110.076455

Donaldson SB, West CM, Davidson SE, Carrington BM, Hutchison G, Jones AP, Sourbron SP, and Buckley DL. (2010) A comparison of tracer kinetic models for T1-weighted dynamic contrast-enhanced MRI: application in carcinoma of the cervix. Magn Reson Med. 63:691-700. 10.1002/mrm.22217

Dreicer R (1997) Metastatic prostate cancer: assessment of response to systemic therapy. Semin Urol Oncol 15:28–32

Durie BG (2006) The role of anatomic and functional staging in myeloma: description of Durie/Salmon plus staging system. Eur J Cancer 42:1539–1543. doi:10.1016/j.ejca.2005.11.037

Durie BG, Salmon SE (1975) A clinical staging system for multiple myeloma Correlation of measured myeloma cell mass with presenting clinical features, response to treatment, and survival. Cancer 36:842–854

Eisenhauer EA, Therasse P, Bogaerts J, Schwartz LH, Sargent D, Ford R, Dancey J, Arbuck S, Gwyther S, Mooney M, Rubinstein L, Shankar L, Dodd L, Kaplan R, Lacombe D, Verweij J (2009) New response evaluation criteria in solid tumours: revised RECIST guideline (version 1.1). Eur J Cancer 45:228–247

Eustace S, Tello R, DeCarvalho V, Carey J, Wroblicka JT, Melhem ER, Yucel EK (1997) A comparison of whole-body turboSTIR MR imaging and planar 99mTc-methylene diphosphonate scintigraphy in the examination of patients with suspected skeletal metastases. Am J Roentgenol 169: 1655–1661

Even-Sapir E, Metser U, Mishani E, Lievshitz G, Lerman H, Leibovitch I (2006) The Detection of Bone Metastases in Patients with High-Risk Prostate Cancer: 99mTc-MDP Planar Bone Scintigraphy, Single- and Multi-Field-of-View SPECT, 18F-Fluoride PET, and 18F-Fluoride PET/CT. J Nucl Med 47:287–297

Galasko CS (1995) Diagnosis of skeletal metastases and assessment of response to treatment. Clin Orthop Relat Res:64–75

Ghanem N, Uhl M, Brink I, Schafer O, Kelly T, Moser E, Langer M (2005) Diagnostic value of MRI in comparison to scintigraphy, PET, MS-CT and PET/CT for the detection of metastases of bone. Eur J Radiol 55:41–55

Ghanem N, Altehoefer C, Kelly T, Lohrmann C, Winterer J, Schafer O, Bley TA, Moser E, Langer M (2006) Whole-body MRI in comparison to skeletal scintigraphy in detection of skeletal metastases in patients with solid tumors. In Vivo 20:173–182

Gosfield E 3rd, Alavi A, Kneeland B (1993) Comparison of radionuclide bone scans and magnetic resonance imaging in detecting spinal metastases. J Nucl Med 34:2191–2198

Groves AM, Beadsmoore CJ, Cheow HK, Balan KK, Courtney HM, Kaptoge S, Win T, Harish S, Bearcroft PW, Dixon AK (2006) Can 16-detector multislice CT exclude skeletal lesions during tumour staging? Implications for the cancer patient. Eur Radiol 16:1066–1073

Gu J, Khong PL, Wang S, Chan Q, Law W, Zhang J (2011) Quantitative assessment of diffusion-weighted MR imaging in patients with primary rectal cancer: correlation with FDG-PET/CT. Mol Imaging Biol. 13:1020–1028. doi: 10.1007/s11307-010-0433-7

Gutzeit A, Doert A, Froehlich JM, Eckhardt BP, Meili A, Scherr P, Schmid DT, Graf N, von Weymarn CA, Willemse EM, Binkert CA (2010) Comparison of diffusion-weighted whole body MRI and skeletal scintigraphy for the detection of bone metastases in patients with prostate or breast carcinoma. Skeletal Radiol 39:333–343

Hamaoka T, Madewell JE, Podoloff DA, Hortobagyi GN, Ueno NT (2004) Bone imaging in metastatic breast cancer. J Clin Oncol 22:2942–2953

Hanrahan CJ, Christensen CR, Crim JR (2010) Current concepts in the evaluation of multiple myeloma with MR imaging and FDG PET/CT. Radiographics 30:127–142. doi: 10.1148/rg.301095066

Hawighorst H, Libicher M, Knopp MV, Moehler T, Kauffmann GW, Kaick G (1999) Evaluation of angiogenesis and perfusion of bone marrow lesions: role of semiquantitative and quantitative dynamic MRI. J magn reson imaging 10: 286–294

Hillengass J, Wasser K, Delorme S, Kiessling F, Zechmann C, Benner A, Kauczor HU, Ho AD, Ho AD, Ho AD, Goldschmidt H, Moehler TM (2007) Lumbar bone marrow microcirculation measurements from dynamic contrast-enhanced magnetic resonance imaging is a predictor of event-free survival in progressive multiple myeloma. Clin Cancer Res 13:475–481. doi:10.1158/1078-0432.CCR-06-0061

Hillengass J, Fechtner K, Weber MA, Bauerle T, Ayyaz S, Heiss C, Hielscher T, Moehler TM, Egerer G, Neben K, Ho AD, Kauczor HU, Delorme S, Goldschmidt H (2010) Prognostic significance of focal lesions in whole-body magnetic resonance imaging in patients with asymptomatic multiple myeloma. J Clin Oncol 28:1606–1610. doi: 10.1200/JCO.2009.25.5356

Horger M, Claussen CD, Bross-Bach U, Vonthein R, Trabold T, Heuschmid M, Pfannenberg C (2005) Whole-body low-dose multidetector row-CT in the diagnosis of multiple myeloma: an alternative to conventional radiography. Eur J Radiol 54:289–297. doi:10.1016/j.ejrad.2004.04.015

Horger M, Weisel K, Horger W, Mroue A, Fenchel M, Lichy M (2011) Whole-body diffusion-weighted MRI with apparent diffusion coefficient mapping for early response monitoring in multiple myeloma: preliminary results. Am J Roentgenol 196:W790–W795. doi:10.2214/AJR.10.5979

Hwang S, Panicek DM (2007) Magnetic resonance imaging of bone marrow in oncology, Part 2. Skeletal Radiol 36: 1017–1027. doi:10.1007/s00256-007-0308-4

Juweid ME, Stroobants S, Hoekstra OS, Mottaghy FM, Dietlein M, Guermazi A, Wiseman GA, Kostakoglu L, Scheidhauer K, Buck A, Naumann R, Spaepen K, Hicks RJ, Weber WA, Reske SN, Schwaiger M, Schwartz LH, Zijlstra JM, Siegel BA, Cheson BD (2007) Use of positron emission tomography for response assessment of lymphoma: consensus of the Imaging Subcommittee of International Harmonization Project in Lymphoma. J Clin Oncol 25:571–578. doi:10.1200/JCO.2006.08.2305

Kershaw LE, Cheng HL (2010) Temporal resolution and SNR requirements for accurate DCE-MRI data analysis using the AATH model. Magn Reson Med 64:1772–1780. doi: 10.1002/mrm.22573

Khoo MM, Tyler PA, Saifuddin A, Padhani AR (2011) Diffusion-weighted imaging (DWI) in musculoskeletal MRI: a critical review. Skeletal Radiol 40:665–681. doi: 10.1007/s00256-011-1106-6

Koh DM, Takahara T, Imai Y, Collins DJ (2007) Practical aspects of assessing tumors using clinical diffusion-weighted imaging in the body. Magn Reson Med Sci. 6:211–224

Komori T, Narabayashi I, Matsumura K, Matsuki M, Akagi H, Ogura Y, Aga F, Adachi I (2007) 2-[Fluorine-18]-fluoro-2-deoxy-D-glucose positron emission tomography/computed tomography versus whole-body diffusion-weighted MRI for detection of malignant lesions: initial experience. Ann Nucl Med 21:209–215

Kwee TC, Fijnheer R, Ludwig I, van Quarles Ufford HM, Uiterwaal CS, Bierings MB, Takahara T, Nievelstein RA (2010) Whole-body magnetic resonance imaging, including diffusion-weighted imaging, for diagnosing bone marrow involvement in malignant lymphoma. Br J Haematol 149:628–630. doi:10.1111/j.1365-2141.2010.08093.x

Langsteger W, Heinisch M, Fogelman I (2006) The role of fluorodeoxyglucose, 18F-dihydroxyphenylalanine, 18F-choline, and 18F-fluoride in bone imaging with emphasis on prostate and breast. Semin Nucl Med 36:73. doi:10.1053/j.semnuclmed.2005.09.002

Lecouvet FE, De Nayer P, Garbar C, Noel H, Malghem J, Maldague BE, Vande_Berg BC (1998a) Treated plasma cell lesions of bone with MRI signs of response to treatment: unexpected pathological findings. Skeletal Radiol 27:692–695

Lecouvet FE, Vande Berg BC, Michaux L, Malghem J, Maldague BE, Jamart J, Ferrant A, Michaux JL (1998b) Stage III multiple myeloma: clinical and prognostic value of spinal bone marrow MR imaging. Radiology 209:653–660

Lecouvet FE, Malghem J, Michaux L, Maldague B, Ferrant A, Michaux JL, Vande Berg BC (1999) Skeletal survey in advanced multiple myeloma: radiographic versus MR imaging survey. Br J Haematol 106:35–39

Lecouvet FE, Dechambre S, Malghem J, Ferrant A, Vande Berg BC, Maldague B (2001) Bone marrow transplantation in patients with multiple myeloma: prognostic significance of MR imaging. Am J Roentgenol 176:91–96

Lecouvet FE, Geukens D, Stainier A, Jamar F, Jamart J, d'Othee BJ, Therasse P, Berg BV, Tombal B (2007) Magnetic resonance imaging of the axial skeleton for detecting bone metastases in patients with high-risk prostate cancer: Diagnostic and cost-effectiveness and comparison with current detection strategies. J Clin Oncol 25:3281–3287

Lecouvet FE, VandeBerg BC, Malghem J, Omoumi P, Simoni P (2009) Diffusion-weighted MR imaging: adjunct or alternative to T1-weighted MR imaging for prostate carcinoma bone metastases? Radiology 252:624. doi:10.1148/radiol.2522090263

Lecouvet FE, Simon M, Tombal B, Jamart J, Vande Berg BC, Simoni P (2010) Whole-body MRI (WB-MRI) versus axial skeleton MRI (AS-MRI) to detect and measure bone metastases in prostate cancer (PCa). Eur Radiol. 10.1007/s00330-010-1879-3

Lee KC, Sud S, Meyer CR, Moffat BA, Chenevert TL, Rehemtulla A, Pienta KJ, Ross BD (2007) An imaging biomarker of early treatment response in prostate cancer that has metastasized to the bone. Cancer Res 67:3524–3528. doi:10.1158/0008-5472.CAN-06-4236

Li WF, Hou SX, Yu B, Li MM, Ferec C, Chen JM (2010) Genetics of osteoporosis: accelerating pace in gene identification and validation. Hum Genet 127:249–285. doi:10.1007/s00439-009-0773-z

Libshitz HI, Hortobagyi GN (1981) Radiographic evaluation of therapeutic response in bony metastases of breast cancer. Skeletal Radiol 7:159–165

Luboldt W, Kufer R, Blumstein N, Toussaint TL, Kluge A, Seemann MD, Luboldt HJ (2008) Prostate carcinoma: diffusion-weighted imaging as potential alternative to conventional MR and 11C-choline PET/CT for detection of bone metastases. Radiology 249:1017–1025

Messiou C, Cook G, deSouza NM (2009) Imaging metastatic bone disease from carcinoma of the prostate. Br J Cancer 101:1225–1232. doi:10.1038/sj.bjc.6605334

Messiou C, Collins DJ, Giles S, de Bono JS, Bianchini D, de Souza NM (2011) Assessing response in bone metastases in prostate cancer with diffusion weighted MRI. Eur Radiol 21:2169–2177. doi:10.1007/s00330-011-2173-8

Montemurro F, Russo F, Martincich L, Cirillo S, Gatti M, Aglietta M, Regge D (2004) Dynamic contrast enhanced magnetic resonance imaging in monitoring bone metastases in breast cancer patients receiving bisphosphonates and endocrine therapy. Acta Radiol 45:71–74

Moulopoulos LA, Dimopoulos MA, Weber D, Fuller L, Libshitz HI, Alexanian R (1993) Magnetic resonance imaging in the staging of solitary plasmacytoma of bone. J Clin Oncol 11:1311–1315

Moulopoulos LA, Dimopoulos MA, Alexanian R, Leeds NE, Libshitz HI (1994) Multiple myeloma: MR patterns of response to treatment. Radiology 193:441–446

Moynagh MR, Colleran GC, Tavernaraki K, Eustace SJ, Kavanagh EC (2010) Whole-body magnetic resonance imaging: assessment of skeletal metastases. Semin Musculoskelet Radiol 14:22–36. doi:10.1055/s-0030-1248703

Nakanishi K, Kobayashi M, Takahashi S, Nakata S, Kyakuno M, Nakaguchi K, Nakamura H (2005) Whole body MRI for detecting metastatic bone tumor: comparison with bone scintigrams. Magn Reson Med Sci. 4:11–17

O'Connor JP, Jackson A, Parker GJ, Jayson GC (2007) DCE-MRI biomarkers in the clinical evaluation of antiangiogenic and vascular disrupting agents. Br J Cancer 96:189–195. doi:10.1038/sj.bjc.6603515

Oyama N, Akino H, Kanamaru H, Suzuki Y, Muramoto S, Yonekura Y, Sadato N, Yamamoto K, Okada K (2002) 11C-acetate PET imaging of prostate cancer. J Nucl Med 43:181–186

Padhani AR (2011) Diffusion magnetic resonance imaging in cancer patient management. Semin Radiat Onco 21:119–140. doi:10.1016/j.semradonc.2010.10.004

Padhani AR, Koh DM (2011) Diffusion MR imaging for monitoring of treatment response. Magn Reson Imaging Clin N Am 19:181–209. doi:10.1016/j.mric.2010.10.004

Parker GJ, Barker GJ, Tofts PS (2001) Accurate multislice gradient echo T(1) measurement in the presence of non-ideal RF pulse shape and RF field nonuniformity. Magn Reson Med 45:838–845

Pollen JJ, Witztum KF, Ashburn WL (1984) The flare phenomenon on radionuclide bone scan in metastatic prostate cancer. Am J Roentgenol 142:773–776

Reischauer C, Froehlich JM, Koh DM, Padevit C, John H, Binkert CA, Boesiger P, Gutzeit A (2010) Bone metastases from prostate cancer: assessing treatment response by using diffusion-weighted imaging and functional diffusion maps–initial observations. Radiology 257:523–531. doi:10.1148/radiol.10092469

Russell WJ, Yoshinagah Antoku S, Mizuno M (1966) Active bone marrow distribution in the adult. Br J Radiol 39:735–739

Ryan SP, Weinberger E, White KS, Shaw DW, Patterson K, Nazar-Stewart V, Miser J (1995) MR imaging of bone marrow in children with osteosarcoma: effect of granulocyte colony-stimulating factor. Am J Roentgenol 165:915–920

Savelli G, Maffioli L, Maccauro M, De Deckere E, Bombardieri E (2001) Bone scintigraphy and the added value of SPECT (single photon emission tomography) in detecting skeletal lesions. Qua J Nuclear Med 45:27–37

Scher HI (2003) Prostate carcinoma: defining therapeutic objectives and improving overall outcomes. Cancer 97: 758–771. doi:10.1002/cncr.11151

Scher HI, Morris MJ, Basch E, Heller G (2011) End points and outcomes in castration-resistant prostate cancer: from clinical trials to clinical practice. J Clin Oncol 29:3695–3704. doi:10.1200/JCO.2011.35.8648

Schmidt GP, Schoenberg SO, Schmid R, Stahl R, Tiling R, Becker CR, Reiser MF, Baur-Melnyk A (2007) Screening for bone metastases: whole-body MRI using a 32-channel system versus dual-modality PET-CT. Eur Radiol 17: 939–949

Schmidt GP, Reiser MF, Baur-Melnyk A (2009) Whole-body MRI for the staging and follow-up of patients with metastasis. Eur J Radiol 70:393–400. doi:10.1016/j.ejrad.2009.03.045

Shankar LK, Hoffman JM, Bacharach S, Graham MM, Karp J, Lammertsma AA, Larson S, Mankoff DA, Siegel BA, Van den Abbeele A, Yap J, Sullivan D (2006) Consensus recommendations for the use of 18F-FDG PET as an indicator of therapeutic response in patients in National Cancer Institute Trials. J Nucl Med 47:1059–1066

Shreve PD, Grossman HB, Gross MD, Wahl RL (1996) Metastatic prostate cancer: initial findings of PET with 2-deoxy-2-[F-18] fluoro-D-glucose. Radiology 199:751–756

Smith A, Wisloff F, Samson D (2006) Guidelines on the diagnosis and management of multiple myeloma 2005. Br J Haematol 132:410–451. doi:10.1111/j.1365-2141.2005.05867.x

Sonpavde G, Pond GR, Berry WR, de Wit R, Eisenberger MA, Tannock IF, Armstrong AJ (2011) The association between radiographic response and overall survival in men with metastatic castration-resistant prostate cancer receiving chemotherapy. Cancer 117:3963–3971. doi:10.1002/cncr.25982

St Lawrence K, Lee TY, Henkelman M (1998) Spatial localization combining projection presaturation with a two-dimensional excitation pulse. Magn Reson Med 40: 944–947

Sugawara Y, Fisher SJ, Zasadny KR, Kison PV, Baker LH, Wahl RL (1998) Preclinical and clinical studies of bone marrow uptake of fluorine-1-fluorodeoxyglucose with or without granulocyte colony-stimulating factor during chemotherapy. J Clin Oncol 16:173–180

Sundaram M, McGuire MH (1988) Computed tomography or magnetic resonance for evaluating the solitary tumor or tumor-like lesion of bone? Skeletal Radiol 17:393–401

Suzuki H, Hasegawa Y, Terada A, Ogawa T, Hyodo I, Suzuki M, Nakashima T, Tamaki T, and Nishio M. (2008) Limitations of FDG-PET and FDG-PET with computed tomography for detecting synchronous cancer in pharyngeal cancer. Arch Otolaryngol Head Neck Surg 134:1191–1195. 10.1001/archotol.134.11.1191

Tateishi U, Gamez C, Dawood S, Yeung HW, Cristofanilli M, Macapinlac HA (2008) Bone metastases in patients with metastatic breast cancer: morphologic and metabolic monitoring of response to systemic therapy with integrated PET/CT. Radiology 247:189–196. doi:10.1148/radiol.2471070567

Terpos E, Moulopoulos LA, Dimopoulos MA (2011) Advances in imaging and the management of myeloma bone disease. J Clin Oncol 29:1907–1915. doi:10.1200/JCO.2010.32.5449

Therasse P, Arbuck SG, Eisenhauer EA, Wanders J, Kaplan RS, Rubinstein L, Verweij J, Van Glabbeke M, van Oosterom AT, Christian MC, Gwyther SG (2000) New guidelines to evaluate the response to treatment in solid tumors. European Organization for Research and Treatment of Cancer, National Cancer Institute of the United States, National Cancer Institute of Canada. J Natl Cancer Inst 92:205–216

Tofts PS, Brix G, Buckley DL, Evelhoch JL, Henderson E, Knopp MV, Larsson HB, Lee TY, Mayr NA, Parker GJ, Port RE, Taylor J, Weisskoff RM (1999) Estimating kinetic parameters from dynamic contrast-enhanced T(1)-weighted MRI of a diffusable tracer: standardized quantities and symbols. J mag reson imaging 10:223–232

Tombal B, Rezazadeh A, Therasse P, Van Cangh PJ, Vande Berg B, Lecouvet FE (2005) Magnetic resonance imaging of the axial skeleton enables objective measurement of tumor response on prostate cancer bone metastases. Prostate 65:178–187

Vande Berg BC, Lecouvet FE, Michaux L, Ferrant A, Maldague B, Malghem J (1998a) Magnetic resonance imaging of the bone marrow in hematological malignancies. Eur Radiol 8:1335–1344

Vande Berg BC, Malghem J, Lecouvet FE, Maldague B (1998b) Classification and detection of bone marrow lesions with magnetic resonance imaging. Skeletal Radiol 27: 529–545

Vande Berg BC, Lecouvet FE, Galant C, Maldague BE, Malghem J (2005) Normal variants and frequent marrow alterations that simulate bone marrow lesions at MR imaging. Radiol Clin North Am 43:761–770. doi:10.1016/j.rcl.2005.01.007

Venkitaraman R, Cook GJ, Dearnaley DP, Parker CC, Khoo V, Eeles R, Huddart RA, Horwich A, Sohaib SA (2009) Whole-body magnetic resonance imaging in the detection of skeletal metastases in patients with prostate cancer. J Med Imaging Radiat Oncol 53:241–247. doi:10.1111/j.1754-9485.2009.02070.x

Vermoolen MA, Kersten MJ, Fijnheer R, van Leeuwen MS, Kwee TC, Nievelstein RA (2011) Magnetic resonance imaging of malignant lymphoma. Expert Rev Hematol 4:161–171. doi:10.1586/ehm.11.17

Vinholes J, Coleman R, Eastell R (1996) Effects of bone metastases on bone metabolism: implications for diagnosis, imaging and assessment of response to cancer treatment. Cancer Treat Rev 22:289–331

Wu X, Kellokumpu-Lehtinen PL, Pertovaara H, Korkola P, Soimakallio S, Eskola H, Dastidar P (2011) Diffusion-weighted MRI in early chemotherapy response evaluation of patients with diffuse large B-cell lymphoma—a pilot study: comparison with 2-deoxy-2-fluoro-D-glucose-positron emission tomography/computed tomography. NMR Biomed 10.1002/nbm.1689

Yang HL, Liu T, Wang XM, Xu Y, Deng SM (2011). Diagnosis of bone metastases: a meta-analysis comparing (18)FDG PET, CT, MRI and bone scintigraphy. Eur Radiol 10.1007/s00330-011-2221-4

Yankeelov TE, Rooney WD, Li X, Springer CS, Jr (2003) Variation of the relaxographic "shutter-speed" for transcytolemmal water exchange affects the CR bolus-tracking curve shape. Magn Reson Med 50:1151–1169. doi: 10.1002/mrm.10624

Young H, Baum R, Cremerius U, Herholz K, Hoekstra O, Lammertsma AA, Pruim J, Price P (1999) Measurement of clinical and subclinical tumour response using [18F]-fluorodeoxyglucose and positron emission tomography: review and 1999 EORTC recommendations. European Organization for Research and Treatment of Cancer (EORTC) PET Study Group. Eur J Cancer 35: 1773–1782